Advanced ASDEX Upgrade pellet guiding system design

B. Ploeckl[a1], H. Köhnlein[1], T.M.J. Engelhardt[2], A. Herrmann[1], P.T. Lang[1] and ASDEX Upgrade Team [b]

1) Max Planck Institut für Plasma Physik, Boltzmannstr. 2, 85748 Garching, Germany

2) Hochschule Coburg, Friedrich-Streib-Straße 2, 96450 Coburg, Germany

Abstract:

Cryogenic pellet injection will be the prime candidate to fuel future fusion power plants. In order to harvest optimum fuelling performance it is essential to inject pellets from the magnetic high field side of the tokamak. The pellet launching system of the tokamak ASDEX Upgrade injects cryogenic hydrogen pellets with a speed of up to 1000 m/s from the magnetic high field side via curved guiding tubes. Pellets passing the guiding tube are sliding on a gas cushion, generated by the Leidenfrost effect. The actual track has a rectangular cross section and is composed of a series of ellipses in order to generate the required 270° looping type turn; the path length is 17 m. The last part of this track is marked by strong geometrical constraints from vacuum vessel port. The previous design was composed by a sequence of three sections of ellipses too, tangentially constant but discontinuous with regard to the curvature. It had been in operation for almost 20 years. Its steps in curvature are supposed to limit the system performance. A novel and advanced geometry concept, adopting a method well-known from civil engineering (e.g. for railroad track design), has been applied to develop an improved design. It relies on clothoid shape sections keeping the track curvatures continuous and thus provide a smooth transition between all the elements. The new design presented improved the pellet launching system performance on ASDEX Upgrade and provides knowledge for an advanced design of pellet guiding tubes in future fusion devices.

1. Introduction

The ASDEX Upgrade centrifuge pellet launching system is in operation for more than 25 years [1]. After some years of operation, the need to inject pellets from the magnetic high field side of the Tokamak was identified [2], [3]. Hence, the looping shaped guiding tube was established and is in operation since [4]. Many experiments for plasma fuelling as well as for ELM pacing have since then been performed showing excellent performance [5]. It is obvious, that the performance of such guiding tube has a big impact on the over-all efficiency of the fuelling system in future fusion devices. Thorough investigations have been performed in view of ITER [6] [7] serving as basis for the preparation of EU-DEMO fuelling system as well as experiences on ASDEX Upgrade. [8]

A water leak occurred during bake-out of the plasma vessel of ASDEX Upgrade and has generated a lot of aggressive steam, which has condensed particularly on colder areas like vessel ports [9]. One of these ports hosts the last section of the guiding tube feeding pellets to the magnetic high field side of the plasma.

The aggressive steam caused severe damage to the vessel structures and unfortunately to the HELICOFLEX seals of many ports. When replacing these gaskets, massive corrosion of the guiding tube has been observed and the need to replace it was recognized. In order to maintain pellet operation, the system was smoothed out as much as possible. Nevertheless, the need to create a new structure was obvious.

---

[a] Corresponding author: bernhard.ploeckl@pp.mpg.de
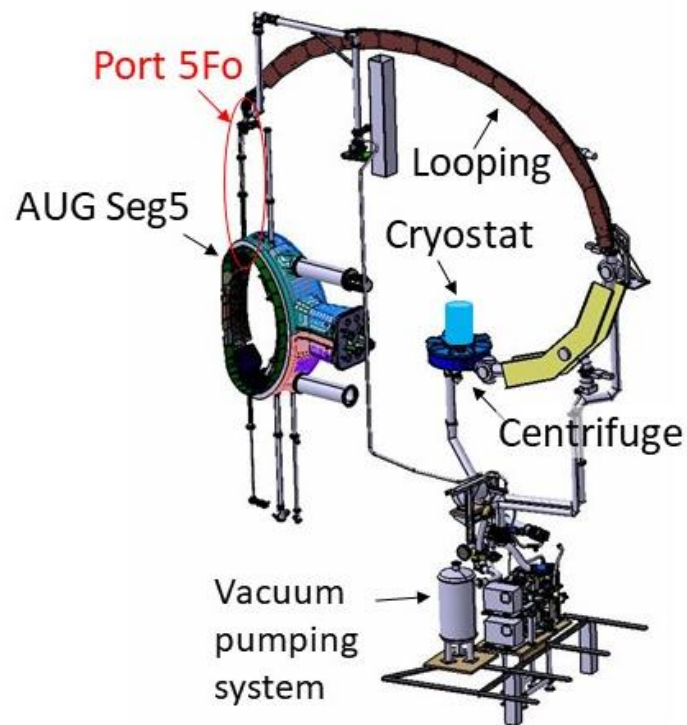[b] For full author list see: H. Meyer et al. 2019 Nucl. Fusion 59 112014

Fig. 1: Pellet injection system composed of cryostat unit, centrifuge launcher, looping shaped guiding tube and vacuum system located in Seg 5. of the ASDEX Upgrade vessel. The replaced part of the pellet guiding system is located in the port 5Fo.

2. Analysis of existing looping geometry

The geometry of the guiding tube was designed to minimize mechanical loads on the pellet due to centrifugal forces and wall contact. Thorough investigations have been carried out to estimate the angular scatter at the exit of the centrifuge and the corresponding forces while hitting the wall. A complex funnel geometry was elaborated and tested in order to keep the injection angle below 2° at a speed of 1000 m/s [10]. The subsequent geometry follows a set of ellipses, which should almost have the same curvature between the end of one and the beginning of another [4].

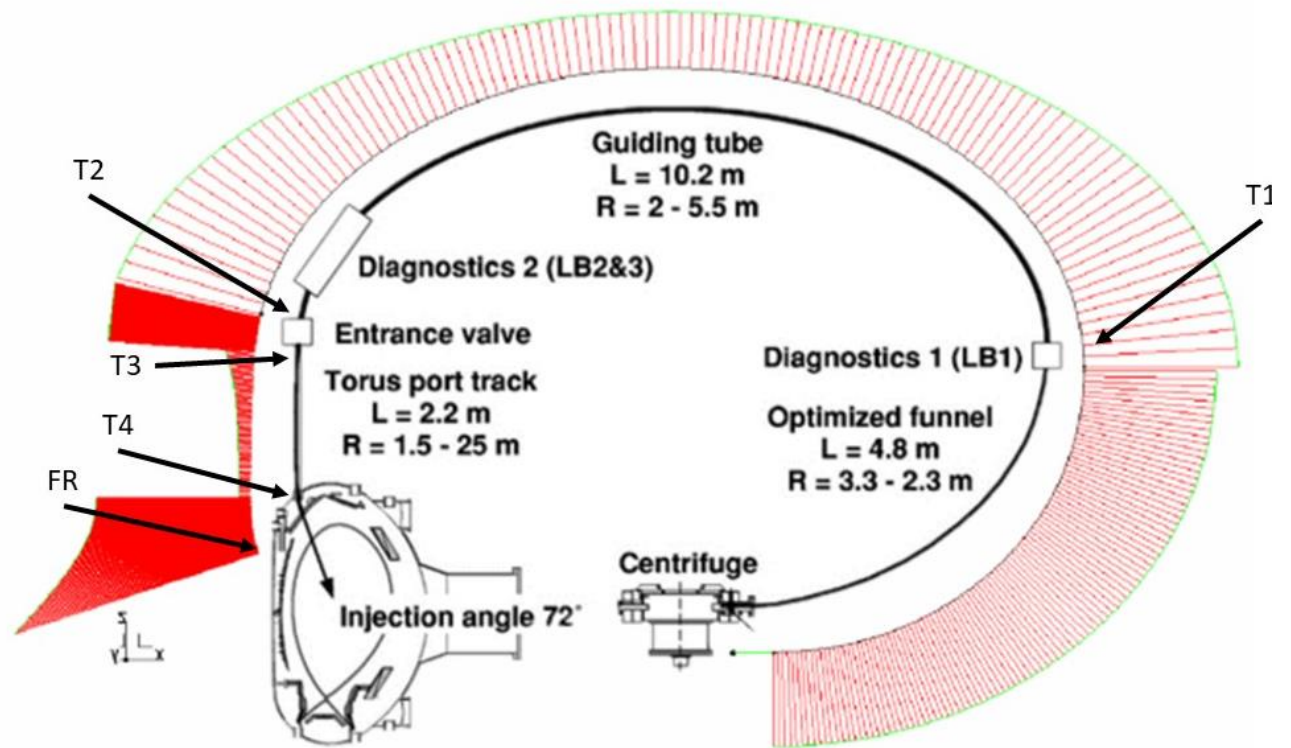Analysing the curvatures is clearly showing that there are steps on the interfaces between the ellipses.

Fig. 2: Analysis of curvature for existing looping geometry. The length of the needles is proportional to the value of the curvature. The density of them corresponds to the supporting points of the CAD analysis, being different for the segments. The transitions between the ellipses are clearly visible. The numbering corresponds to those presented in **Table 1**. In particular in the torus port track section the geometrical constraints were difficult to tackle. This section consists of a sequence of 3 ellipses.

The first transition, between the funnel and the upper part of the loop, provides a moderate transition from R_{out}=2.33 m to R_{in}=1.99 m, which is considered feasible. A free flight section with a gap of 41 mm between these two segments is present, enabling the separation of both parts by a gate valve.
The second transition provides a very good accordance of the curvature, having a step of about 1% of radius.
Transition 3 multiplies the radius by a factor of 5 from 2.1 m up to 10 m.
The last transition in turn reduces the radius drastically by a factor of 13 from 25 m down to 1.998 m, which is considered to put unfavourable load to the pellet. The abrupt nature of this curvature change creates additional forces due to big accelerations at that point.

Transition	R_{out} [m] Pellet leaving out of guiding tube	R_{in} [m] Pellet entering the guiding tube	Step (R_{out}/R_{in})
T1 (LB1)	2.33	1.99	1.1709
T2 (Entrance valve)	2.093	2.073	1.0096
T3	2.101	10.007	0.2100
T4	25.978	1.998	13.0020
FR (Final radius)	1.200		

Table 1: Radii at the transitions from one ellipse to the other and the relative change. Positions see **Fig. 2**.

The mechanical load on the pellet depends on its geometry, speed and curvature radius. For a cubic pellet, the stress due to external forces σ_c can be calculated:

$$\sigma_c = \frac{\rho \, l \, v^2}{R} \qquad (1)$$

Using density ρ, pellet length l, speed v and curvature radius R.

Calculating the pressure on a 1.9 mm pellet for R_{min}=1.2 m and a speed of 1000 m/s, this yields a value of 0.317 MPa. This pressure is at the upper limit of what the yield strength can endure, taking the data range provided in the literature for hydrogen and still in the middle of the range for deuterium. That is why any

improvement on the geometry is considered useful to increase pellet survival probability and decrease mass loss due to erosion.

Isotope	Density [g/cm³]	Yield strength [MPa]	Valid at temperature [K]
H	0.087	0.35 0.07	4.2 12
D	0.20	0.53 0.21	4.2 16.4
T	0.32	1.03	8

Table 2: Material properties for hydrogen isotopes [11]

3. Presentation of new concept

Providing a smooth path even in bends at high speed is a task of daily routine in civil engineering, designing motorways or railroad tracks [12] [13]. The task is to provide a smooth transition between straight and circular segments. Direct crossover from straight to circular track creates load swings, resulting in reduced convenience for passengers and in case of railway increased wear and tear on rails and waggons.

Fig. 3: Railway track (Open Street Maps)

Fig. 4 Motorway track (Open Street Maps)

One method to tackle this issue is to introduce clothoids, aka cornu spiral. The basic principle is to add transition segments between straight and circular sections with continuously increasing curvature.
The curvature R is calculated:

$$R = \frac{A^2}{L} \qquad (2)$$

With L: length of path (L>0); A: scaling factor

3.1. Design steps for clothoids

The first step is to measure the angle τ between the tangent on start and end of element, see Fig. 5.

Fig. 5: Tangents on beginning and end of a bend

The second step is to determine the minimum bend radius R according to material and or geometrical constraints. The material properties provide the yield strength. This defines the minimal radius R for a given pellet speed.

In a third step the length of the track is estimated:
$$L = 2\,R\,\tau \qquad (3)$$
Finally, the scaling factor is calculated using the formula:
$$A^2 = L\,R \qquad (4)$$
In order to obtain the track from normalized clothoid function:
$$X = x\,A;\; Y = y\,A \qquad (5)$$

The Port 5Fo is very narrow, using gaps between toroidal field (TF) coils. Starting point of the design is a free flight section passing the torus gate valve of AUG, hence pellets are moving straight ahead with some angular scatter (~1°). The transition to the straight section in the middle of the vertical port is using 5 clothoid segments. The final bend to the initial injection point is resulting in three clothoid segments. The guiding tubes ends at the same point and with same angle in upper divertor region as the initial track.

No.	Type	τ[rad]	L [mm]	A	R1 [mm]	R2 [mm]	Length of path [mm]
1	Straight				∞	∞	9.78
2	Clothoid 1	0.0130435	60	371.48	∞	2300	60
3	Clothoid 2	1.086956522	5000	3391.16	2300	2400	208.58
4	Circle				2400	2400	20.96
5	Clothoid 3	1.041666667	5000	3464.1	2400	2500	200.18
6	Clothoid 4	0.02	100	500	2500	18000	86.11
7	Circle				18000	18000	333.4
8	Clothoid 5	0.006111	220	1989.97	18000	∞	220
9	Straight				∞	∞	168.53
10	Clothoid 6	0.0044444	160	1697.05	∞	18000	160
11	Circle				18000	18000	217.1
12	Clothoid 7	0.0833333	200	489.9	18000	1200	189.8
13	Circle				1200	1200	195.7
14	Clothoid 8	0.0625	150	424.26	1200	∞	150
15	Straight				∞	∞	0.2

Table 3: Parameters of geometrical elements of new track (in direction of flight).τ, L and A are defining the clothoid, R1 is the starting radius, R2 the end radius. The length of path, indicated in the last column, specifies the used length of the clothoid. This is in case of combining two clothoids, e.g. due to place restrictions (e.g. No.2 and No.3). In cases where the full clothoid is used (transition from straight to circle or vice versa), the values for L and length of path are identical.

The coordinates of the geometry are derived from the normalized clothoid function using the parameters displayed in Table 3 and then imported to CATIA.
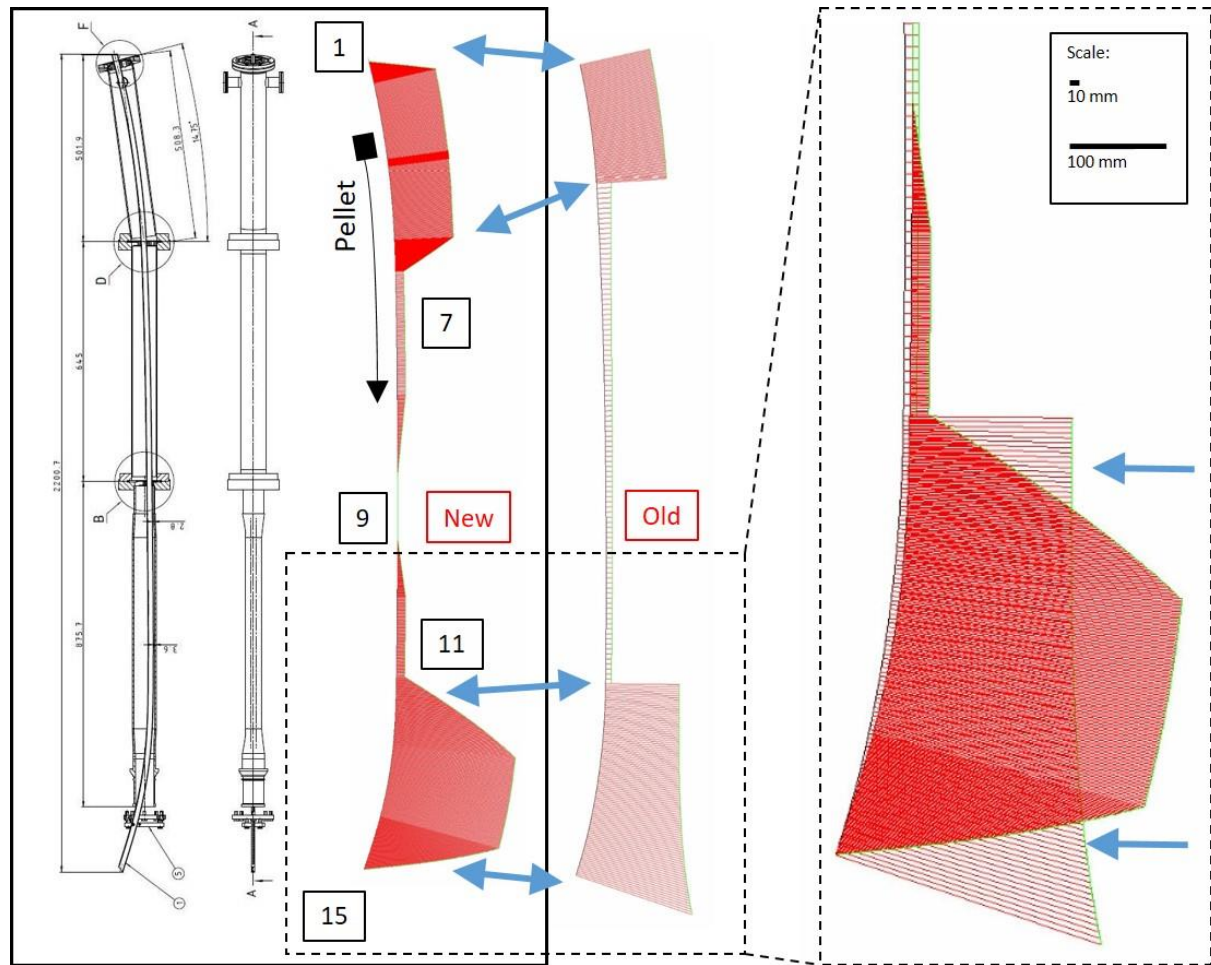
Fig. 6: Engineering drawing of the port 5Fo access tube into the AUG torus vessel with the new torus port track integrated (left, two side views shown). Curvature analysis in CATIA of the new track (middle) in comparison to the old one (right), showing a significant improvement of transitions between the geometrical elements. In particular, no steps in curvature are present anymore. The numbers are referring to the geometrical elements listed in **Table 3**.The value of the maximal curvature is about the same since geometrical boundary conditions (point in space and angle of entrance and exist) are kept. A detailed view of the last segment is showing both tracks and the corresponding curvatures. The track using clothoids needs more space to get the same position and direction.

4. Design of guiding tube

The first guiding tube segment in port 5Fo (torus port track in Fig. 2) was a complex structure. Mainly manufactured from aluminium, the slide way was covered by a CuBe- foil in order to get a very smooth surface. Due to the narrow installed-space-related conditions, the part has to be disassembled prior to mounting and dismounting. This is of course unfavourable. The aim of the new design is to enable installation in one part and to minimize the manufacturing effort providing the same smooth surface.

The existing looping geometry (guiding tube in Fig. 2) at ASDEX Upgrade [10] is using a microwave guiding tube, slotted at the inner side in order to provide proper pumping capability for the removal of the evaporated pellet material. This is essential to avoid the presence of gas accumulation that applies high heat load to the pellet and has the potential to generate gas blocking. This design has been working well already for a couple of years and is considered suitable for the guiding tube in port 5Fo as well. Microwave guiding tubes need a very smooth surface in order to reduce microwave power losses. The surface roughness was found to be $R_z = 1.88 \, \mu m$ and $R_a = 0.11 \, \mu m$ (HOMMEL-ETAMIC T8000). The size is WR51 (inner dimensions: 6.48 mm x 12.95 mm), made from oxygen free copper (OF-Cu). The tube in the looping section was made of WR42 (inner dimensions 10.67 mm x 4.21 mm). The gate valve from the vacuum vessel separates the looping from the in-vessel part inside port 5Fo. The guiding tube of the looping ends in front of the gate valve, those of the port 5Fo starts after this valve; hence, there is a free flight section in between. In the free flight section, pellets are moving straight ahead with a scatter of about 1° around the last tangent on the looping guiding tube. The following section inside the port 5Fo has a wider cross section (lateral 4.2 mm → 6.48 mm and upright 10.67 mm → 12.95 mm). Thus,

all pellets are introduced into the guiding tube after the free flight section. The first segment of the guiding tube is straight in order to fit to the initial movement of the pellets.

The old guiding tube in port 5Fo was completely open on the inner side, apart from having some small beams ensuring mechanical integrity. In order to provide proper pumping capability, the microwave guiding tubes were perforated with ~300 holes having a diameter of 3.5 mm in a distance of 6 mm. This leads to a level of transparency of ~20%. In comparison, the looping section guiding tube has a transparency of 10%.

Pellet movement inside guiding tubes can be regarded as a multi wall collision process with a scattering angle of about 1 °. Hence, in straight sections or even sections with a huge radius the pellet can detach from the outer side of the guiding tube and can hit the opposite (inner) side. These segments are carefully identified and excluded from being equipped with holes. Hitting a hole will destroy the pellet immediately. A pellet that strikes the inner part of the tube leaves this surface with the same angle and moves back to the outer side. The transition from the straight section to a curved one should consider this fact and avoid an impact velocity bigger than the critical impact speed of $v_{\perp cr}$=45 m/s [10]. Due to existing geometrical constraints in port 5Fo and the absence of alternative trajectories, this was not analysed in detail for this project. However, for new designs this is highly recommended. In particular, many activities have been launched for EU-DEMO in order to tackle this issue in an early design stage [8].

During bake out of the vessel of ASDEX Upgrade, the port 5Fo will be heated up to 150 °C. The thermal expansion of the port and the guiding tube will be different in particular during heat up and cool down phase due to different temperature gradients. In flat top phase, the difference will not be significant, as the expansion coefficient of copper and stainless steel is in the same range.

The fixed bearing is located on the vessel (lower) side of the port; all other fixations are designed as loose bearings. Great care has been taken to enable the option to install this part in one piece and without the need to dismount parts of the badly accessible port 5Fo. The bearings are made from Torlon (Polyamide-imide), a thermoplastic polymer with excellent properties under vacuum conditions even at elevated temperature during bake-out.

5. Manufacturing/installation

The manufacturing is composed from two main steps. First step is applying the holes for evaporation and second bending the tube to the right shape. The drilling task is the first one in order to make profit of the straight shape of the tube (not yet bent). The bending process is easier due to the removed material on the inner side of the tube. The tube has been bent using a template and the resulting shape is verified using a gauge with a milled groove (Fig. 7).
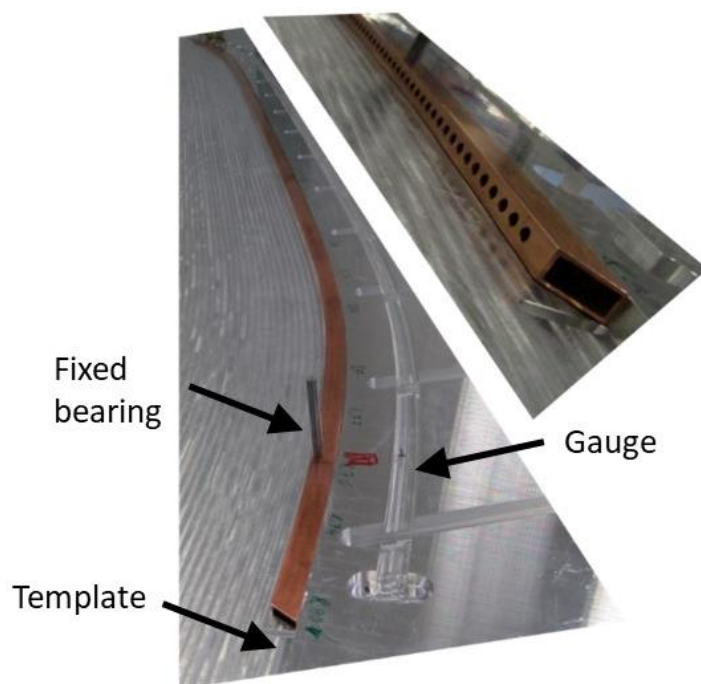

Fig. 7: Template and gauge for manufacturing and test of guiding tube. The bolt marks the fixed bearing at the lower part of the tube. The template and gauge has been made using NC milling machines as well as the original track; hence, the geometric tolerances are in the same range (±0.1mm).

This device can be mounted from the vessel side in one part with the loose bearings already mounted at their place. The fixed bearing defines the position of the tube exit with respect to the components of the upper divertor. In the future, a modified geometry for the new upper divertor for ASDEX Upgrade is envisaged. The present design will enable the easy exchange of the guiding tube to a new one adapted to the new divertor geometry.

6. Results

After installation and commissioning of the system, the new setup showed very good performance. There are two parameters, which are relevant for assessment: the pellet survival probability and the mass loss during transfer.

The survival probability is defined as ratio of fired pellets to arrived ones. Pellets can break in guiding tube due to unfavourable geometry, which causes strong forces, or minor quality due to inhomogeneity in the ice rod.

The mass loss is the ratio of the initial pellet particle content, derived from the geometry to the particles arrived at the plasma calculated by the density increase after pellet injection.

We compare three cases: (i) the initial geometry investigated just after bringing the looping guiding system first into service; (ii) the situation after the steam leak with strong corrosion, but already cleaned as much as possible; (iii) the new build set up with novel geometry.

Fig. 8 shows the result; the initial geometry data indicate a dependence on the pellet speed, with a stronger decay for speed above 880 m/s. Using the corroded guiding tube, experiments with pellet speed 240 m/s and 540 m/s were performed. No speed dependence was found, but a strong reduction of the survival probability: from initial 0.88-0.95 it drops down to 0.65 in this speed range.

Using the new set up with clothoid shape, a set of experiments were carried out during restart of ASDEX Upgrade. 16 pellets were injected during 3 shots with v_p=240 m/s, 186 pellets in 6 shots with v_p=560 m/s and 28 pellets in 5 shots with v_p=820 m/s. The usual pellet speed for dedicated fuelling experiments on ASDEX Upgrade is 560 m/s; hence there are more data available than for the other two speeds. The other experiments were performed piggyback and due to the short time window with just a small number of pellets.

The results are much improved. The survival probability is in the range of 0.85 up to 0.93, increasing with higher speed. With respect to the error bars, a constant value is possible as well. Surprisingly, at a speed of 440 m/s, the performance drops to about 0.25. The reason is not fully understood, some resonance vibrations may be present. Unfortunately, just a couple of experiments were performed with this speed and no data from the previous setup is available. Furthermore, no data is available for the speed range 1000 m/s with the new setup. At this speed, the increased mass loss overcompensates the better fuelling performance due to the deeper penetration at that high speed in this given setup. Hence, there were no experiments carried out at this speed for a long time at ASDEX Upgrade.
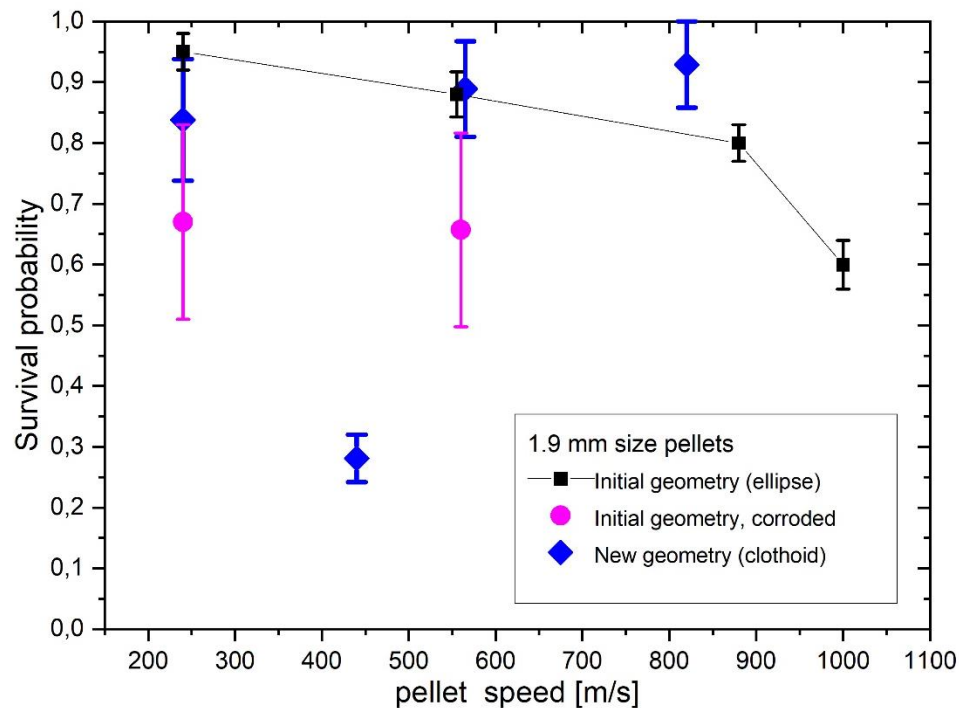

Fig. 8: Survival probability of pellets through the looping and the port 5Fo. The initial values are from [1], the corroded are data collected in the campaign 2017 and the new ones in the campaign 2019/2020.

The survival probability is the most obvious parameter that contributes to the overall efficiency of a pellet guiding system. The mass loss is an additional parameter, which allows a more sensitive assessment. The overall mass loss during the way through the guiding system is relevant as well, as it applies to all pellets and is present for all pellets, even at a survival probability of 100 %. Nevertheless, both parameters are relevant, the survival probability is more relevant to the plasma control issues, for a holistic view on the fuel cycle, the mass loss is perhaps more relevant.

Mechanical load on the pellet causes some mass loss and this load depends on the pellet speed (with a power of 2), see above. The aim of the new design is to minimize this load on the pellet; the results show a clear progress compared to the initial design. The mass loss increase with the speed, but weaker than before. The nominal pellet speed for the design of pellet launching systems in future fusion devices is usually determined after an optimisation process taking in to account the fuelling efficiency of the pellets on the plasma. The main parameters for this optimization are the injection location and – angle as well as the pellet speed. Now, there is a method on hand in order to design a sound guiding tube geometry.

The mass transfer efficiency for the novel set up was investigated during the start-up of the AUG 2019/20 campaign where a dedicated commissioning phase for the pellet system was included. During this commissioning phase, all different operational modes of the entire pellet launching system have been tested, in particular all the different available pellet sizes and speeds. The particle content of the pellet arriving was regarded as measure for the transferred mass fraction, taking the ideal particle contend of a perfectly shaped pellet as a reference. In this approach, the transferred mass fraction is the ratio of pellet particles arriving in the plasma per ideal pellet particle content. To be noted, since already during the initial test bed characterisation of the launcher centrifuge it was found [1] even at the centrifuge exit arrive only about 85% of the ideal mass, a transferred mass ratio of 0.85 indicates for an essentially perfect loss free transfer through the guiding system. To determine the pellet particle content in the plasma, it would be required to measure the plasma particle content immediately before and just after pellet arrival. However, this is not possible directly. The plasma particle content for a given time requires integration over a suitable full density profile. Because this yields highest accuracy, we took the profiles measured for the electron density by a set of different diagnosing tools; integration providing the plasma electron contend N_e. Since we can assume pure D pellets, this refers exactly to the amount of D atoms carried by the pellets. Due to the limited temporal resolution of the diagnostics tools involved, the available N_e data do not provide sufficient accuracy to calculate the real pellet size. This lack of resolution can be partially overcome by analysing the data provided by the DCN laser interferometer. These data turned out more suitable to depict the enhancement of the plasma density after pellet arrival with higher resolution in magnitude and time. However, albeit the enhanced temporal resolution of about 1 ms still prompt particle losses caused by drift effects and the triggering of edge-localised modes cannot be resolved. Furthermore, for such a measurement only the information on the line-averaged density along an observation chord can be derived, represented by the value $\overline{n_e}$. To calibrate now the signal $\overline{n_e}$ available at the needed temporal resolution to the signal N_e providing the desired quantity, a correlation analysis has been performed. Here, data were taken at times both values are available during post-pellet phases for cases representing again all the pellet sizes and speeds. The result obtained is displayed in Fig. 9, plotting $\overline{n_e}$ versus N_e. Obviously; both quantities show a correlation sufficiently close to a linear one such the calibration can be achieved by a simple scaling factor. As represented by the fit function (blue line in figure), the pellet particle amount deposited inside the confined plasma (within the last closed flux surface - LCFS) about 1 ms after the pellet ablation can be calculated by $N_e = 10 \times \overline{n_e}$ [m^{-3}]. Since our experiments were performed in a stable type-I ELMy H-mode plasma scenario by applying ample auxiliary heating, prompt particle losses were assumed to remove already about half of the ablated particles as typical for such conditions [14]. Taking pellet ensembles containing typically 100 single pellets, this way the transferred mass fraction as plotted in Fig. 10 were obtained. For each set, compiled for a specific speed and the largest pellet size, the mean value and the variation (FWHM) is provided.
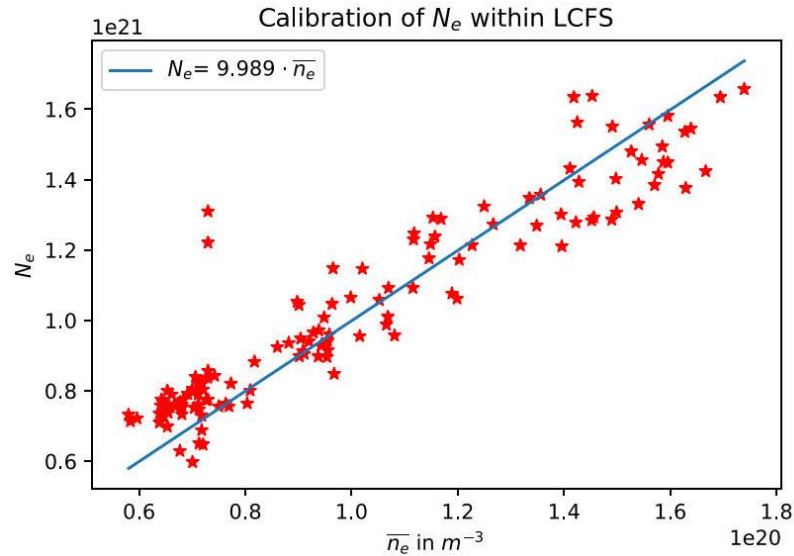
Fig. 9: Pellet induced enhancements measured by the DCN laser interferometer for the line-averaged density versus increase in plasma particle inventory for time points with a full density profile available. Data cover pellets ranging from smallest to largest size and slowest to highest speeds. The line represents the fit taken to derive mass transfer fractions.
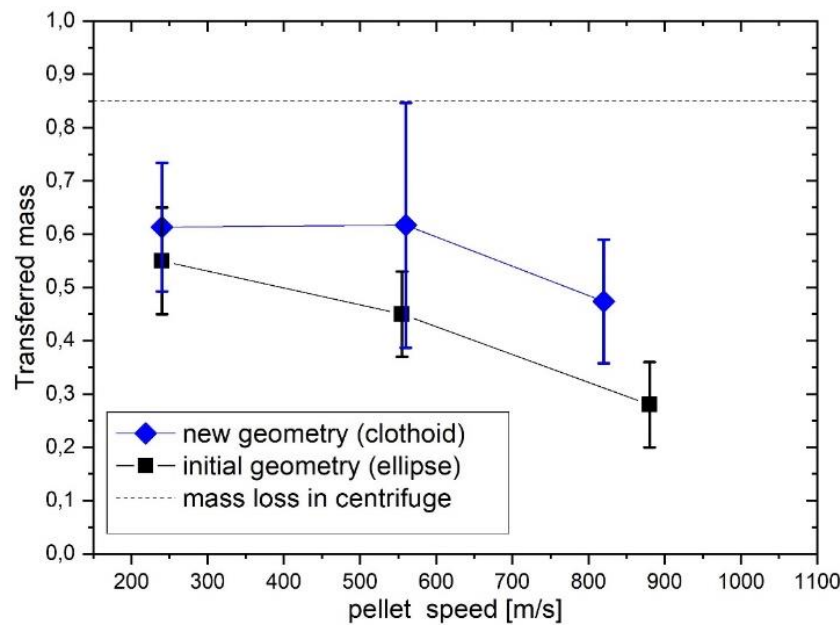

Fig. 10: Transferred mass for pellet during travel from the pellet source to the plasma indicated for initial geometry using ellipses and new geometry using clothoids. The mass loss in the pellet centrifuge is considered 0.15%. It is obvious, that the new geometry shows a better performance in particular at higher speeds. This is in good agreement with the analysis of the curvatures of the two geometries. The new geometry has no steps in curvature; hence, the load on the pellet is lower, in particular for higher speeds. The mass loss is considered a good indicator regarding the mechanical load on the pellet within the limits of its material properties. Increasing mass losses indicate that the conditions are very close to this limit.

7. Summary

We present a new design concept, already widely in use for civil engineering and railway design activities. These rules allow minimizing the overall mass loss of the pellet launching system and thus improving the system performance. The mass loss does not just burden the vacuum system, which have to pump away the lost material. The latter does not serve for fuelling and the next pellet must compensate a missing one, which is a challenge to the density control system as well.

The use of HF-waveguides is an economically and technically feasible option to realize such complex and precise geometries. Manufacturing these geometries is challenging and costly, using templates for bending and verification facilitates the task.

The good performance of the new system encourages to put more emphasis to the design of future pellet guiding tube systems as well as to implement R&D activities for optimizing this part of the fuel cycle of a future fusion power plant.

Acknowledgments

Data availability statement

Raw data were generated at the ASDEX Upgrade facility. Derived data supporting the findings of this study are available from the corresponding author upon reasonable request.

References

[1] C. Andelfinger, E. Buchelt, P. Cierpka, H. Kollotzeck, P. T. Lang, R. S. Lang, G. Prausner, F. X. Söldner, M. Ulrich and G. Weber, "A new centrifuge pellet injector for fusion experiments," *Rev. of Sc. Instr.,* vol. 64, pp. 983-989, 1993.

[2] P. T. Lang, K. Büchl, M. Kaufmann, R. S. Lang, V. Mertens, H. W. Müller, J. Neuhauser, ASDEX Upgrade team and NI Team, "High-Efficiency Plasma Refuelling by Pellet Injection from the Magnetic High-Field Side into ASDEX Upgrade," *Phys. Rev. Letters,* vol. 8, pp. 1487-1490, 25 August 1997.

[3] H. W. Müller, K. Büchl, M. Kaufmann, P. T. Lang, R. S. Lang, A. Lorenz, M. Maraschek, V. Mertens and J. Neuhauser, "High- β Plasmoid Drift during Pellet Injection into Tokamaks," *Phys. Rev. Lett.,* vol. 83, p. 2199, 1999.

[4] P. T. Lang, P. Cirepka, O. Gehre, M. Reich, C. Wittmann, A. Lorenz, D. Frigione, S. Kalvin, G. Kocsis, ASDEX Upgrade Team and S. Maruyama, "A system for cryogenic hydrogen pellet high speed inboard launch," *Rev. of Sci. Instr.,* vol. 74, pp. 3974-3983, 2003.

[5] B. Ploeckl and P. T. Lang, "The enhanced ASDEX Upgrade pellet centrifuge launcher," *Rev. of Sci. Instr.,* vol. 84, p. 103509, 2013.

[6] S.K. Combs et al., "Pellet delivery and survivability through curved guide tubes," *Fus. Eng. Design,* Vols. 75-79, pp. 691-696, 2005.

[7] S. K. Combs, L. R. Baylor, S. J. Meitner, J. B. Caughman, D. A. Rasmussen and S. Maruyama, "Overview of recent developments in pellet injection for ITER," *Fusion Engineering and Design,* vol. 87, p. 634–640, 2012.

[8] P. T. Lang, F. Cismondi, C. Day, E. Fable, A. Frattolillo, C. Gliss, F. Janky, B. Pégourié and B. Ploeckl, "Optimizing the EU-DEMO pellet fuelling scheme," *Fus. Eng. Des.,* 2020.

[9] V. Rohde, A. Herrmann, M. Balden, D. Bösser, K. Hunger, G. Schall, M. Uhlmann, T. Vierle and ASDEX Upgrade Team, "Recovery from a hot water leakage at the Tokamak ASDEX Upgrade," *Fus. Eng. Des.,* vol. 157, 2020.

[10] A. Lorenz, P. T. Lang and R. S. Lang, "Impact strength of cryogenic deuterium pellets for injection," *Rev. Sci. Instr.,* vol. 71, no. 10, p. 3736, October 2000.

[11] S. K. Combs and L. R. Baylor, "Pellet-Injector Technology—Brief History and Key Developments," *FUSION SCI TECHNOL,* vol. 73, pp. 493-518, May 2018.

[12] A. Kobryń, Transition Curves for Highway Geometric Design, Springer Nature, 2017.

[13] E. Bachmann, "Die Klothoide als Übergangskurve im Straßenbau," *Schweizerische Zeitschrift für Vermessung und Kulturtechnik,* 12 Juni 1951.

[14] P. T. Lang, H. Zohm, K. Buchl, C. F. J., O. Gehre, O. Gruber, V. Mertens, H. W. Muller and J. Neuhauser, "Pellet fuelling of ELMy H mode discharges on ASDEX Upgrade," *Nucl. Fusion,* vol. 36, p. 1531, 1996.